Eur. Phys. J. B **39**, 131–137 (2004)
DOI: 10.1140/epjb/e2004-00178-9

THE EUROPEAN PHYSICAL JOURNAL B

Steady high viscosity liquid micro-jet production and fiber spinning using co-flowing gas conformation

A.M. Gañán-Calvo[a], M. Pérez-Saborid, J.M. López-Herrera, and J.M. Gordillo

Escuela Superior de Ingenieros, Universidad de Sevilla, Camino de los Descubrimientos s/n, 41092 Sevilla, Spain

Received 1st October 2003 / Received in final form 21 March 2004
Published online 18 June 2004 –

Abstract. Here we propose a new physical approach to the high-speed conformation of a Newtonian viscous liquid into a fiber (high speed fiber drawing), which suppresses all well-known axisymmetric and asymmetric instabilities during the fiber drawing. Our approach is based on the application of an appropriate gas pressure profile along the viscous jet or fiber axis, provided by a special subsonic micro-nozzle concentric with the fiber. The micro-nozzle design and optimization is mathematically provided.

PACS. 47.15.Gf Low-Reynolds-number (creeping) flows – 47.15.Fe Stability of laminar flows – 47.27.Wg Jets

1 Introduction

The generation of fibers from very viscous liquid precursors is an ancient and increasingly growing activity of mankind, and involves enormous global revenues. From polymer fiber production used in the huge-market textile industry, to the more recent optical fiber drawing processes, handling a highly viscous fluid to form a long, thin and uniform fiber is as common as ubiquitous. In general, current industrial processes are optimized by means of a few process approaches (classical hot drawing-used by the large optical fiber companies-, and direct extrusion through a hole), imposed in many cases by a secular inertia. Drawing of glass fibers is typically dominated by viscous forces modified by heating and cooling the molten threadline. The classical fiber drawing present several well known limitations and problems. In particular, under appropriate conditions, perturbations introduced in the threadline lead to an axisymmetric instability referred to as draw resonance (see e.g. [1–3] and references therein). The draw resonance sets on when the draw ratio $E = V_1/V_o$ exceeds a value close to 20 (V_o and V_1 are the input and the output velocities in the threadline) and manifest itself as a self-sustained oscillation of the cross sectional radius of the drawn fiber or, in other words, as a propagating wave of swelling and contractions. Although heat removal from the threadline, which increases the viscosity of the molten liquid, stabilizes the spinning process leading to a significant increase in the threshold value E, draw resonance imposes a severe limit for the drawing velocity V_1 under currently required high-speed productivities [4]. When a high speed gas stream is used to shear the surface of the molten highly viscous liquid and to extract the fibers, it is impossible with currently available techniques to precisely control the fiber diameter and the whipping instabilities (violent lateral motion) of the fibers, which make them difficult to handle. Besides, direct extrusion from "bushings" (cavities holding the melted glass) exerts strong shear stresses on the fiber while it is drawn through the orifice in the bushing, and often presents expensive maintenance problems and clogging. Also, some other interesting instabilities appearing when extruding a non-Newtonian liquid through a capillary have been described in [5,6].

Here we propose a general methodology and process for a Newtonian high viscosity liquid fiber — e.g. a glass — to (i) provide a perfect control on the fiber diameter, (ii) suppress the speed limits of the hot fiber drawing process owing to *instabilities*, and (iii) overcome the high shear stresses and clogging problems of direct extrusion. In this work, we aim to show that these three difficult technological challenges can be accomplished by a new physical approach which defines an entirely new fiber drawing process as here proposed.

2 The newly proposed fiber drawing process

Our suggested process involves drawing the fibre (either from a preform or from a bushing) concentrically surrounded by a carefully shaped subsonic gas flow trough a special small nozzle (see Fig. 1). A preform is a solid rod, with a much larger diameter than the final fiber, which is introduced in a region where it is heated up to the yield point and above to produce the drawn fiber. The gas flow imposes an appropriate steady pressure distribution

[a] e-mail: alfonso@eurus2.us.es

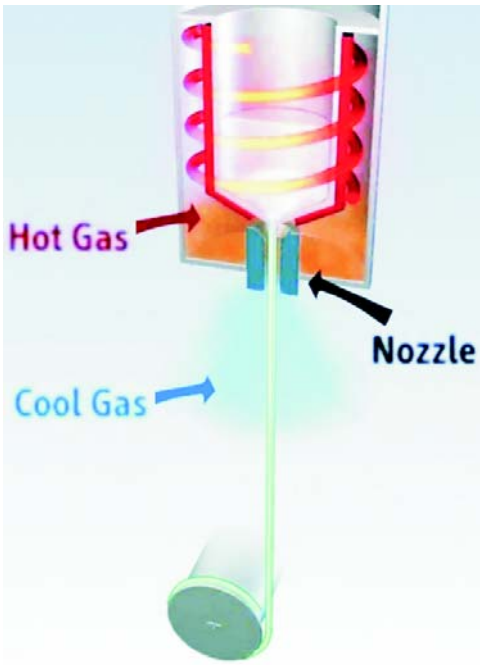

Fig. 1. Proposed experimental set-up.

around the fiber while it is drawn. The important features of this co-flow combination are: (i) the gas pressure distribution on the fiber can be calculated to suppress instabilities for *any fiber drawing velocity* (which means a theoretically *unlimited* increase in productivity); and (ii) the shear stress on the fiber can be reduced to a minimum (this allows the controlled production of complex and fragile fiber structures, hollow fibers, photonic bandgap fibers [8], etc.). Our method would improve not only fiber uniformity and stability but also would provide a precise control on the fiber temperature profile and internal structure (avoiding diffusion, crystallization, etc.). First, in optical fiber manufacturing, the fiber quenching time controls the amount of undesired crystallization of the fiber bulk, that can be precisely engineered by the gas co-flow (or "sheath" flow) temperature profile since the convective heat transfer coefficient can become dominant over radiation by the sheath flow. This means that the gas temperature distribution along the nozzle would be very rapidly transferred to the drawn fiber, providing the means for a simple and accurate control on the fiber temperature profile. Secondly, the sheath gas flow may be used to control the chemicals surrounding the fiber that may diffuse into it. These two issues would additionally imply a significant improvement of the amorphous structure of the fiber and its eventual clarity limit [7]. Additionally, the gas pressure drop along the nozzle results in a very simple feedback control parameter to mitigate any possible small, long term fiber diameter variation associated to possible external thermal oscillations or material inhomogeneities (see for example [4] for fiber diameter feedback control in high speed fiber drawing), without the need to stop the process, to change the extrusion nozzle or the drawing speed. Finally, since the fiber diameter is significantly smaller than the micro-nozzle internal diameter, that fiber diameter can be changed within a certain size range without the need to change the micro-nozzle.

One of the main issues of this work is to show how the well-known fiber drawing instability which limits the maximum drawing speed, the so-called draw resonance instability, can be suppressed just establishing a proper pressure profile along the liquid molten threadline. This can be accomplished if one surrounds the fiber by a gas environment. Obviously, since a variable pressure distribution imposes a gas stream co-flowing with the liquid theadline, this stream provokes a tangential stress on the liquid interface and an enhanced heat transfer from the liquid to the gas. We will focus our attention on the benefits of using an optimized pressure distribution along the threadline, limiting ourselves to the ranges in which the collateral (but beneficial) effects of the tangential stress and the heat transfer on the dynamics of the thread line can be neglected.

As it will be shown below, the fiber spinning is a process in which viscous forces in the liquid generally dominate over the rest, namely, inertia, surface tension, and gravity forces. This is particularly true for drawing velocities V_1 of the order of 0.5 m/s and below, which is typically the velocity achieved in most of the current industrial processes. However, it should be pointed out that in the case of ultra-high speed drawing (V_1 above 20 m/s), the inertia forces may become important and, consequently, its effects should be considered in the analysis. In the proposed method, this would be the case if the imposed gas pressure drop were large enough to have a non negligible fraction of that pressure drop employed on building up the inertia of the liquid threadline. In the present work, we restrict ourselves to moderate drawing velocities, typically below 5 m/s, for which the process can still be assumed viscosity-dominated. The analysis taking into account the liquid inertia, important for large withdrawal velocities, will be considered in future works.

3 Formulation of the problem

We consider a Newtonian liquid concentrically drawn through a small nozzle with length L, and surrounded by a gas stream as sketched in Figure 1. Assuming an axisymmetric configuration (the effect of asymmetries will be subsequently discussed), the liquid hydrodynamics obeys the Navier-Stokes equations, which in cylindrical coordinates read

$$\begin{aligned} &U_R + V_X + U/R = 0 \\ &\rho(U_T + U\,U_R + V\,U_X) = -P_R + (2\mu U_R)_R \\ &\qquad + [\mu(U_X + V_R)]_X + 2\mu(U_R - U/R)/R \\ &\rho(V_T + V\,V_R + V\,V_X) = -P_X + g \\ &\qquad + (2\mu V_X)_X + [\mu R(U_X + V_R)]_R/R, \end{aligned} \tag{1}$$

where U and V are the radial and the axial components of the velocity, respectively, P is the liquid pressure and

g is the gravity acceleration (assumed as applied in the x-direction only). T, X and R are the time, the axial and the radial coordinates. μ and ρ are the viscosity and density of the liquid. Subindexes denote differentiation. In addition, the stresses on the interface in the normal and tangential direction must be balanced,

$$P - P_g - \frac{2\mu}{1+F_X^2}[U_R + F_X^2 V_X - (V_R + U_X)F_X] = \frac{\sigma}{(1+F_X^2)^{1/2}}\left(\frac{1}{F} - \frac{F_{XX}}{1+F_X^2}\right),$$
$$\frac{\mu}{1+F_X^2}[2F_X U_r + (1-F_X^2)(V_R+U_X) - 2F_X V_X] = \tau, \tag{2}$$

where F is the position of the interface, P_g is the gas pressure on the interface, σ the liquid surface tension and τ is the tangential stresses exerted by the gas on the liquid column. Finally, the surface must move with the velocity field on the interface,

$$F_T + V F_X - U|_{R=F} = 0. \tag{3}$$

If the variables are expanded in Taylor series with respect to R,

$$V = \overline{V} + V_2\, R^2 + ...$$
$$U = -\overline{V}_X\, R/2 - (V_2)_X\, R^2/4 + ...$$
$$P = \overline{P} + P_2\, R^2 + ..., \tag{4}$$

and the slenderness of the liquid column is taken into account ($a \sim O(R) \ll O(L)$), the following quasi-one-dimensional equations of continuity and axial momentum can be derived from the above equations (see [3,9,10] for details),

$$(F^2)_T + (F^2\overline{V})_X = 0$$
$$\rho F^2[\overline{V}_T + \overline{V}\,\overline{V}_X] = [3\mu F^2 \overline{V}_X]_X + \rho g F^2 - F^2(P_g)_X + \sigma F_X + 2\tau F. \tag{5}$$

The momentum equation, besides the forces exerted by the gas on the liquid, incorporates all the relevant effects, namely, the inertial, viscous, gravitational, and surface tension forces.

Before we proceed with the problem analysis including the initial and boundary conditions, in order to gain some physical intuition on the particular application we are dealing with, it would be illustrative to consider the production of an optical glass fiber with diameter $a = 100\,\mu$m, drawn at a velocity of $V_1 = 3$ m/s through a nozzle of $L = 15$ mm. Assuming that the liquid temperature stays almost constant during the fiber drawing, typical values of the relevant physical constants of the molten glass are $\sigma = 0.250$ mN/m, $\rho = 3000$ Kg/m^3 and $\mu_o = 10^3$ Pa s (which corresponds to a temperature of about 1300 K), where for our purposes here we use $\mu = \mu_o$ as a constant viscosity. If we compare the gravity forces term of the order of $\rho g a^2$, the liquid acceleration term of the order of $\rho a^2 V_1^2/L$ and the surface tension forces term of the order $\sigma a/L$, to the much larger viscous and pressure forces terms of the order of $\mu a^2 V_1/L^2$, we obtain

$$\frac{\text{Gravity Forces}}{\text{Viscous Forces}} \sim \frac{\rho g L^2}{\mu_o V_1} \sim 0.002$$
$$\frac{\text{Accelerat. Forces}}{\text{Viscous Forces}} \sim \frac{\rho V_1 L}{\mu_o} \sim 0.15$$
$$\frac{\text{Surf. Tens. Forces}}{\text{Viscous Forces}} \sim \frac{\sigma L}{\mu_o a V_1} \sim 0.01. \tag{6}$$

Therefore, gravity forces, liquid acceleration and surface tension forces are negligible compared to the much larger viscous and pressure forces.

Let us then define non-dimensional variables $t = T V_1/L$, $x = X/L$, $f = F/a$, $v = \overline{V}/V_1$, $p = P_g/(3\mu_o V_1/L)$ and $f_s = \tau/(3\mu_o V_1 a/L^2)$ standing for the non-dimensional time, axial coordinate, fiber radius, liquid velocity, gas pressure, and axial resultant of the tangential gas surface stresses respectively, where μ_o is a reference liquid viscosity. Based on the above discussion, one can further reduce the equation (5) to:

$$\partial_t f^2 + \partial_x(f^2 v) = 0,$$
$$\partial_x p = \partial_x(\mu/\mu_o f^2 \partial_x v)/f^2 + 2f_s/f \tag{7}$$

with boundary conditions

$$\text{at} \quad x = 0\text{:}\ p = p_o = \frac{LP_o}{3\mu_o V_1},\ f = E^{1/2} \text{ and } v = E^{-1},$$

and

$$\text{at} \quad x = 1\text{:}\ p = p_a = \frac{LP_a}{3\mu_o V_1},\ f = 1 \text{ and } v = 1, \tag{8}$$

where $E = V_1/V_o$, V_o is the intake liquid velocity (or the glass preform velocity in glass fiber drawing); P_o and P_a are the upstream gas stagnation pressure and the external ambient pressure, respectively.

It is worth noting that the higher the liquid viscosity is, the closer the real radial velocity profile is to the flat profile assumed in the quasi-one-dimensional model, since the viscous diffusion time $t_v \sim \rho a^2 \mu_o^{-1}$ is many orders of magnitude smaller than the hydrodynamic time $t_o \sim L V_1^{-1}$ (i.e., $\mu_o L(\rho V_1 a^2)^{-1} \ll 1$).

In general, there is a strong non-linear dependence of the liquid viscosity on temperature Θ_l, $\mu = \mu(\Theta_l)$, following an Arrhenius-type law of the form $\mu(\theta_l)/\mu_o = \zeta = \exp A/(N_A k \Theta_o \theta_l)$, where A is an activation energy, N_A is Avogadro's number, k is Boltzmann constant, $\theta_l = \Theta_l/\Theta_o$, and Θ_o is the upstream gas stagnation temperature. In general, the temperature Θ in the liquid column is given by the equation

$$\rho C[(\Theta_l)_T + U(\Theta_l)_R + V(\Theta_l)_X] = \phi_v + [k_l\, R\,(\Theta_l)_R]_R/R + [k_l(\Theta_l)_X]_X \tag{9}$$

where k_l and C are the thermal conductivity and heat capacity of the liquid, respectively, and ϕ_v is the viscous dissipation work given by

$$\phi_v = \mu\{2[U_R^2 + (U/R)^2 + V_X^2] + (U_X + V_R)^2\}. \tag{10}$$

The energy equation (9) can be further simplified if one keeps in mind that we are dealing with a viscous slender fiber for which the axial velocity profile can be assumed flat. First of all, axial conduction is negligible compared to radial conduction and axial convection is dominant versus radial convection. Secondly, after comparing the dissipation term, of the order of $\mu_o V_1^2/L^2$, to the convection term, of the order of $\rho C \Delta_X \Theta_l V_1/L$ where $\Delta_X \Theta_l$ is the axial variation of temperature, one concludes that dissipation is unimportant. Thus, the local temperature profile is given, in dimensionless form, by

$$v\partial_x \theta_l = \alpha \partial_r (r \partial_r \theta_l)/r \tag{11}$$

with boundary conditions $\theta_l(x, f) = \Theta_s/\Theta_o$ ($\theta_l(x, 0) \neq \infty$) and $\theta_l(0, r) = 1$, where Θ_s is the non dimensional gas temperature at the fiber surface and $\alpha = k_l L/(V_1 \rho C a^2)$. We can distinguish two limiting problems:

1. $\alpha \gg 1$: in this case, we can assume $\theta_l = \Theta_s/\Theta_o$. We call this the "gas limited" (GL) case;
2. $\alpha \ll 1$: in this case, we can assume $\theta_l = 1$. This is the traditional isothermal limit (IT).

In the GL case, the temperature profile of the fiber in the radial direction can be considered uniform, and the temperature is controlled by the ability of the gas to transport the heat through its thermal boundary layer. In the IT limit, the liquid bulk remains at the initial Θ_o temperature because of the inability of the gas thermal boundary layer to evacuate the heat from the liquid.

On the other hand, owing to the disparity of the liquid and the gas particle residence times, the gas can be considered steady for any non-steady liquid motion of interest (including motions with wavelengths of the order of the fiber diameter). Thus, the gas pressure and temperature can be considered as steady variables in the problem, which are functions of the axial coordinate only and can be calculated at any time given the local nozzle and fiber geometries. In addition, the gas flow is governed by the well known isentropic compressible one-dimensional inviscid equations: the gas pressure and temperature distributions are given by their stagnant values P_o and Θ_o, respectively, and the nozzle geometry through $A(x)$, its local cross section area. The gas expansion in the nozzle provokes a change in the gas temperature along the nozzle. Making dimensionless the gas pressure and temperature with their stagnant values, the gas temperature θ_g is given by

$$\theta_g = 1 - \Delta\theta_g = (1 - \Delta p_g)^{(\gamma-1)/\gamma} \tag{12}$$

in the isentropic assumption, where $\gamma = C_p^{(g)}/C_v^{(g)}$ is the adiabatic gas constant, $C_p^{(g)}$ and $C_v^{(g)}$ are the usual gas heat coefficients at constant pressure and density, respectively; and Δp_g and $\Delta\theta_g$ are the pressure and temperature drop at a certain point of the nozzle from its entrance.

Further assumptions must be made in order to properly model the tangential stress exerted by the gas and the heat removed or added from the gas to the liquid threadline.

3.1 Gas boundary layer, viscous shear stress, and heat transfer on the fiber surface. Theoretical assumptions

The gas boundary layer on the liquid jet has a thickness of the order of $\delta \sim L\, Re_g^{-1/2}$ where $Re_g = \rho_g V_g L/\mu_g$ is the Reynolds number of the gas stream, V_g is the gas velocity and, μ_g and ρ_g are the characteristic gas viscosity and density. The thickness of the gas boundary layer is, as a function of the stagnation conditions of the gas,

$$\delta \sim (\mu_g L P_o^{-1})^{1/2} (R_g \Theta_o)^{1/4}, \tag{13}$$

where $R_g = C_p^{(g)} - C_v^{(g)}$ as usual, and we have estimated the gas velocity as $V_g \sim (P_o/\rho_g)^{1/2}$ and the density of the gas as $\rho_g \sim P_o/(R_g \Theta_o)$. The tangential viscous stress τ acting on the jet surface, owing to the much faster gas stream, is then of the order of

$$\tau \sim \mu_g V_g/\delta \sim (\mu_g L^{-1} P_o)^{1/2} (R_g \Theta_o)^{1/4}. \tag{14}$$

Comparing the axial resultant per unit volume of the viscous stress on the surface, F_s, of the order of $F_s \sim \tau/a$, with the extensional (axial) resultant of the viscous stress, F_v, of the order of $F_v \sim \mu_o V_1/L^2$, and since $P_o \sim \mu_o V_1/L$, one obtains

$$F_s/F_v \sim (\mu_g/\mu_o)^{1/2} \left(R_g \Theta_o/V_1^2\right)^{1/4} L/a. \tag{15}$$

We seek for production velocities V_1 much larger than $\mu_g \mu_o^{-1} L^2 a^{-2} (R_g \Theta_o)^{1/2}$ (of the order of about 10^{-3} to 10^{-2} m/s in practical situations), for which $F_s \ll F_v$, and the contribution of the surface stress is negligible versus the axial component of the normal pressure stress, of the order of $P_o L^{-1} \sim \mu_o V_1 L^{-2}$. Thus, the equations in (7) reduce to

$$\begin{aligned} &\partial_t f^2 + \partial_x (f^2 v) = 0, \\ &\partial_x p = \partial_x (\zeta f^2 \partial_x v)/f^2 \end{aligned} \tag{16}$$

where $\zeta = \mu/\mu_o$. Owing to the strong dependence of viscosity with temperature, limited liquid temperature variations (about 5 to 20% of Θ_o in practice) are sufficient to increase the liquid viscosity by orders of magnitude, which is a mechanism suppressing most instabilities in itself. This is why, traditionally, non-isothermal drawing owing to radiation is the way to guarantee fiber shape stability because of the consequent substantial increase in liquid viscosity as the fiber proceeds downstream (the larger the viscosity, the smaller the perturbations growth rate), although it requires a limited production velocity, given by $V_1 \ll k_l L/(\rho C a^2)$ ($\alpha \gg 1$). In our study, in which radiation is assumed absent, non-isothermal drawing is bounded by the GL case, and our method would provide an enhanced fiber stability owing to an enhanced heat removal by the gas sheath. In the GL case, considering a portion of the thread line, its axial temperature variation $\Delta_X \Theta_l$ of the liquid owing to the heat transfer through the gas thermal boundary layer $\delta_T \sim \delta/Pr$ where Pr is the Prandtl number (in reality, $\delta_T \sim \delta$ since

$Pr = \mu_g C_p^{(g)}/k_o \sim O(1)$, k_o being the gas thermal conductivity at temperature Θ_o) is of the order of

$$\rho C V_1 \Delta_X \Theta_l a^2 \sim k_o \frac{\Delta\Theta}{\delta} aL \tag{17}$$

where $\Delta\Theta$ is the transversal variation of the gas temperature across the gas boundary layer. In many practical situations, we have $L(\rho C a V_1)^{-1} k_o \delta^{-1} \ll 1$, for which the heat transfer from the gas to the liquid can be considered negligible, and the liquid can be considered isothermal.

It is worth emphasizing here that the non isothermal drawing stabilizes the fiber since it hardens in the drawing process. However, in this work we will go farther ahead showing that, even in the isothermal limit ($\alpha \ll 1$ or $V_1 \gg k_l L/(\rho C a^2)$), the most unstable and difficult to control case corresponding to high speed and ultra-high speed fiber drawing (more than 20 m/s), our method will suppress the most dangerous source of quality breakdown: the drawing instabilities. Thus, we will focus on this particular limit, also considered by Yarin et al. [3] in the case of simple drawing. We will show that a carefully shaped co-flowing gas stream provide the means to: (i) completely stabilize the fiber; (ii) yield fiber homogeneity and/or shape control, and (iii) a subsequent control on fiber quenching.

4 Suppression of fiber instabilities

Using the above given problem formulation, in this section we present an analysis of the novel proposed process as a way to suppress the fiber drawing instabilities.

4.1 Suppression of the non-symmetric instability (fiber whipping)

As a result of imposing a stream of gas coflowing with the threadline, whipping instabilities are set after the nozzle exit if the gas exit velocities are over a certain *threshold*. These instabilities are related to the shear stresses existing on the interface of two coflowing fluids travelling at different velocities, as in the classical Kelvin-Helmholtz stability analysis (see [11,12]). Several analyses on the influence of a coaxial gas stream on the linear stability of a liquid jet have been carried out ([13–15] among others) and most of them are devoted to determine the droplet size distribution resulting from the jet breakup. In the context of thread-annular flows (a thin cylindrical elastic core surrounded by coflowing fluid), which could resemble more closely the particular conditions of our problem, it has been shown that the Reynolds number and the thread velocity have a significant influence on the unsteady behaviour of the thread [16]. However, an analysis including the effect of an axial gas pressure gradient is, as far as we know, not available.

The existence of this gas velocity threshold can be justified both theoretically and experimentally. First, whipping instabilities at the nozzle exit possess a local absolute nature. These instabilities can be delayed by the liquid viscous forces up to the point that they can be convected downstream, and the whipping disappears. This occurs when the viscous forces per unit volume, of the order of $\mu_o V_1/a^2$, are sufficiently large compared to the local acceleration term, of the order of $\rho V_1/t_c$, where t_c is the characteristic time of the instability (growing time), that can be estimated by setting that the pressure drop in the gas (δp) due to the distortion of the jet surface (δf) accelerates normally the liquid jet:

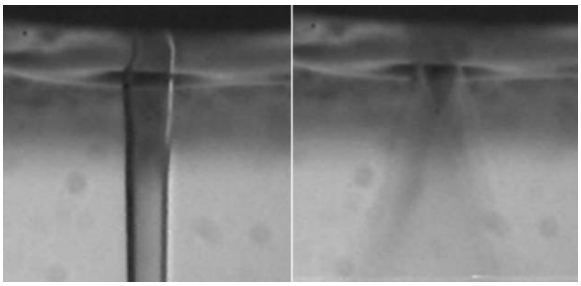

Fig. 2. (a) Photograph of a liquid fiber (viscosity $\mu = 7$ Pa s) of exit diameter 300 μm, drawn through a simple cylindrical orifice of diameter $D = 500$ μm with length $L = 150$ μm, for a gas exit velocity $v_g = 135$ m s^{-1}; (b) $v_g = 150$ m s^{-1}.

$$\delta p_g \sim \rho_g U_g^2 \frac{\delta f}{a} \sim a\rho \frac{\delta v_l}{\delta t} \sim a\rho \frac{\delta^2 f}{\delta t^2} \rightarrow t_c \sim \left(\frac{\rho}{\rho_g}\right)^{1/2} \frac{a}{U_g}, \tag{18}$$

where v_l is velocity component normal to the undisturbed liquid velocity ($\sim V_1$). Thus, the number

$$Re = \frac{(\rho\rho_g)^{1/2} U_g a}{\mu_o} \tag{19}$$

should be smaller than a certain threshold value Re^*. We have made a preliminary series of experiments with glycerol and glucose syrup ($\mu = 0.6$ and 7 Pa s, respectively), see Figure 2, and determined that $Re^* \simeq 0.25$. As far as we know, this is a new result for a co-flowing, concentric and unbounded gas-fiber system at the exit of a small orifice. Thus, we restrict our method to safe values of Re^* below this threshold. We will show in a practical case how this apparently strong restriction does not preclude the existence of a parametrical region where stable "unlimited" high speed fiber drawing is possible. Anyway, a further refined analytical study on the asymmetric fiber instabilities owing to the gas flow would be welcome, but it is out of the practical scope and limited space of this work.

4.2 Nozzle geometry and suppression of the "drawing resonance" axisymmetric instability: The isothermal case

A convergent subsonic nozzle always produce a monotonically decreasing pressure along its axis. Our task is here to obtain a pressure distribution suppressing the axisymmetric instabilities described in [1–3] while minimizing energy

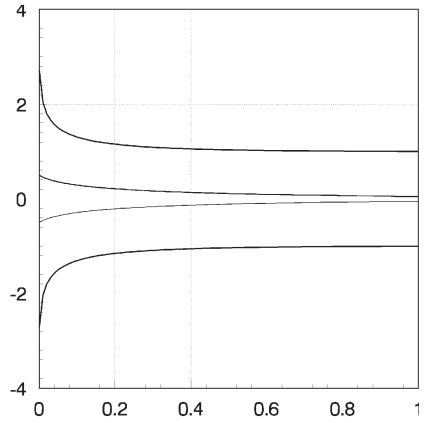

Fig. 3. Cross-section view of the fiber drawn along a nozzle as here proposed. Here, an optimal nozzle shape as discussed in the text is plotted ($\lambda = 5.65$), together with the resulting drawn fiber shape. The external curves represent the nozzle shape, and the internal curves (close to $r = 0$) represent the fiber shape. Arbitrary length x and r scales.

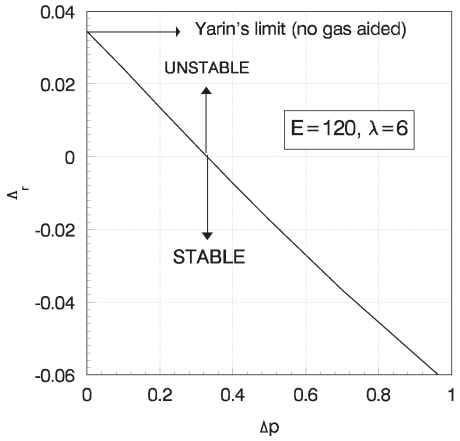

Fig. 4. An example of the stabilization effect of the pressure distribution.

consumption. The parametrical space for optimization of convergent nozzle geometries is in principle infinite; however, gas boundary layer growth and possible separation is reduced with smooth nozzle shapes like the ones producing exponentially decreasing pressure distributions. Thus, in order to reduce the problem of the convergent nozzle geometry to a *single* parameter, without loss of generality on our aimed task, we have reduced the space of possible nozzle geometries to those producing pressure distributions of the type:

$$p(x) - p^* = \Delta p\, e^{-\lambda x} \tag{20}$$

where $\Delta p = p_o - p_a$, $p^* = p_a - \Delta p \exp(-\lambda)$, and λ is a single, real number to parameterize a sufficiently broad family of nozzle geometries. The set of free parameters $\{\Delta p, \lambda\}$ will be optimized for the requirement of an *unlimited* fiber drawing (i.e. fiber production) with a *minimum* energy consumption (minimum Δp). Thus, given a pressure drop Δp, we seek for λ values for which the drawing is absolutely stable for any (unlimited) given productivity (E value).

Now, consider the small axisymmetric perturbations problem given by

$$f(x) = f_e(x)\left[1 + \alpha(x)e^{\Lambda t}\right],\ v(x) = v_e(x)\left[1 + \beta(x)e^{\Lambda t}\right] \tag{21}$$

and governed by equations (16) in the IT limit ($\zeta = 1$), where $f_e(x)$ and $v_e(x)$ are the steady values of the problem for the given boundary conditions (8)

$$\begin{aligned} & f_e^2 v_e = 1 \\ & v_e \frac{\mathrm{d}^2 v_e}{\mathrm{d}x^2} - \left(\frac{\mathrm{d}v_e}{\mathrm{d}x}\right)^2 + \lambda \Delta p\, e^{-\lambda x} = 0 \end{aligned} \tag{22}$$

where $v_e(0) = E^{-1}$ and $v_e(1) = 1$. An example of a solution of the steady equation (22) is depicted in Figure 3 where we plot the shape of the fiber and the geometry of the micro-nozzle which give rise to such fiber shape. The selected exponential decay of the pressure, $\lambda = 5.65$, as will be shown below, allows the suppression of the instabilities. $\alpha(x)$ and $\beta(x)$ are complex functions with argument small compared to 1, and Λ is the complex perturbation growth rate. Pressure variations owing to the fiber section fluctuations are of the order of $O(\alpha a^2/A(x)) \ll O(\alpha)$, and thus will be neglected in the analysis. Thus, α and β are governed by a set of 2 complex ODEs with homogeneous boundary conditions that can be readily obtained from equations (16)

$$\begin{aligned} & 2\alpha\Lambda f_e^2 + \frac{\mathrm{d}(2\alpha + \beta)}{\mathrm{d}x} = 0 \\ & 2\frac{\mathrm{d}^2\alpha}{\mathrm{d}x^2} + 2f_e^2\Lambda\frac{\mathrm{d}\alpha}{\mathrm{d}x} + \beta f_e^2 \lambda \Delta p\, e^{-\lambda x} = 0 \end{aligned} \tag{23}$$

where $\alpha(0) = 0$, $\beta(0) = 0$, and $\alpha(1) = 0$. These equations and boundary conditions determine the eigenvalue Λ, whose real part Λ_r gives the growth factor in time. In Figure 4, we give the value of Λ_r as a function of Δp for $\lambda = 6$ and $E = 120$.

For every given E and λ values, there is a corresponding Δp value above which any axisymmetric instabilities are suppressed. In Figure 5 we plot the curves dividing the $\{E, \Delta p\}$ space into *stable* (above the curve) and *unstable* (below the curve) parametrical sub-spaces, for several λ values of practical interest. One may immediately note from this plot that for every given λ value, there is a particular limiting value of Δp above which the fiber is stable for *any* value of $E > 1$. In Figure 6, we plot these limiting Δp values as a function of λ, and obtain a universal **minimum** value of the pressure above which the fiber is absolutely stable regardless of the fiber productivity E.

A minimum limiting Δp value about 0.33 around the point $\lambda \simeq 5.65$ can be found. In this case, given a desired fiber diameter a and fiber production velocity V_1, the minimum gas pressure drop $P_o - P_a$ necessary to have absolute stability is given by the simple expression:

$$P_o - P_a \simeq \mu_o V_1 / L \tag{24}$$

with a nozzle shape given in Figure 1.

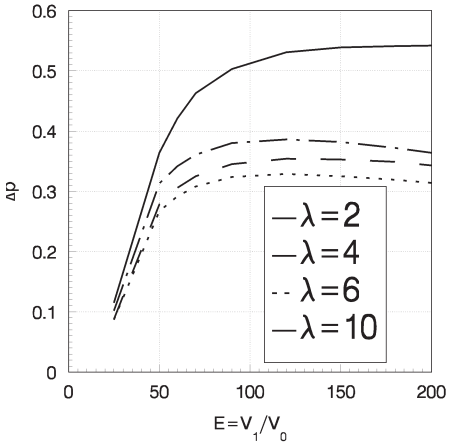

Fig. 5. Stability values of Δp vs. E for several λ values.

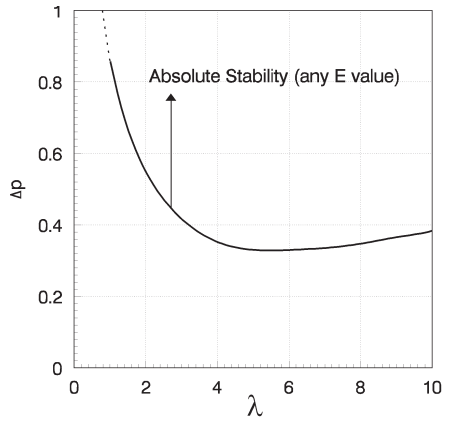

Fig. 6. Absolute stability values of Δp vs. λ.

A further refinement of the nozzle geometry is possible introducing new geometrical parameters (the minimum p_o value may be further optimized). This refinement does not limit the generality of our analysis.

A practical case. Consider the production of 260 km/day of a fiber with a diameter of 100 μm. The glass has viscosity $\mu_o = 10^3$ Pa s at $\Theta_o = 1300$ K ($\rho = 3000$ kg m^{-3}). Since $V_1 = 3$ m s$^{-1} \gg k_l L/(\rho Ca^2) = 0.3$ m s^{-1}, the fiber can be considered quasi-isothermal (IT limit). Using an optimum nozzle geometry with length $L = 15$ mm and a pressure drop $P_o - P_a = 2 \times 10^4$ Pa, both axisymmetric and whipping instabilities can be avoided under our present results since $Re \sim 10^{-2}$ in this case. The minimum theoretical power consumption for gas pressurization is rather low for nozzle sections below a square millimeter, and the heat power depends on the general system lay-out. Scale-up is straightforward.

This work is supported by the Ministry of Science and Technology of Spain, Flow Focusing Inc., and Flow Fiber Inc. in alliance with Battelle Corp. (USA). The authors are grateful to Dr. Pascual Riesco-Chueca for his comments on the work.

References

1. F.T. Geyling, G.M. Homsy, Glass Technol. **21**, 95 (1980)
2. P. Gospodinov, A.L. Yarin, Int. J. Multiphase Flow **23**, 967 (1997)
3. A.L. Yarin, P. Gospodinov, O. Gottlieb, M.D. Graham, Phys. Fluids **11**, 3201 (1999)
4. Z. Yin, Y. Jaluria, ASME J. Heat Transfer **122**, 351 (2000)
5. B. Meulenbroek, C. Storm, V. Bertola, C. Wagner, D. Bonn, W. van Saarloos, Phys. Rev. Lett. **90**, 024502 (2003)
6. V. Bertola, B. Meulenbroek, C. Wagner, C. Storm, A. Morozov, W. van Saaloos, D. Bonn, Phys. Rev. Lett. **90**, 114502 (2003)
7. G.A. Thomas, B.I. Shraiman, P.F. Glodis, M.J. Stephens, Nature **404**, 262 (2000)
8. P. Russell, Science **299**, 358 (2003)
9. J. Eggers, T.F. Dupont, J. Fluid Mech. **262**, 205 (1994)
10. F.J. Garcia, A. Castellanos, Phys. Fluids **8**, 2837 (1996)
11. S. Chandrasekhar, *Hydrodynamic and hydromagnetic stability* (Dover Publications, 1981)
12. P. Drazin, W. Reid, *Hydrodynamic stability* (Cambridge University Press, 1981)
13. C. Weber, Z. Angew. Math. Mech. **11**, 136 (1931)
14. J.B. Keller, S.I. Rubinow, Y.O. Tu, Phys. Fluids **16**, 2052 (1973)
15. J.M. Gordillo, M. Perez-Saborid, A.M. Gañán-Calvo, J Fluid Mech. **448**, 23 (2001)
16. Ch. Frei, P. Lüscher, E. Wintermantel, J. Fluid Mech. **410**, 185 (2000)